Clinical Cancer Research

CDK4/6 Inhibitor as a Novel Therapeutic Approach for Advanced Bladder Cancer Independently of *RB1* Status

Carolina Rubio[1,2], Mónica Martínez-Fernández[1,2,3], Cristina Segovia[1,2,3], Iris Lodewijk[1,3], Cristian Suarez-Cabrera[1], Carmen Segrelles[1,2,3], Fernando López-Calderón[3], Ester Munera-Maravilla[1,3], Mirentxu Santos[1,2,3], Alejandra Bernardini[1,2,3], Ramón García-Escudero[1,2,3], Corina Lorz[1,2,3], Maria José Gómez-Rodriguez[1,2], Guillermo de Velasco[1], Irene Otero[1], Felipe Villacampa[1,2], Felix Guerrero-Ramos[1], Sergio Ruiz[4], Federico de la Rosa[1,2], Sara Domínguez-Rodríguez[5], Francisco X. Real[2,6,7], Núria Malats[2,5], Daniel Castellano[1,2], Marta Dueñas[1,2,3], and Jesus M. Paramio[1,2,3]

Abstract

Purpose: Bladder cancer is a clinical and social problem due to its high incidence and recurrence rates. It frequently appears in elderly patients showing other medical comorbidities that hamper the use of standard chemotherapy. We evaluated the activity of CDK4/6 inhibitor as a new therapy for patients unfit for cisplatin (CDDP).

Experimental Design: Bladder cancer cell lines were tested for *in vitro* sensitivity to CDK4/6 inhibition. A novel metastatic bladder cancer mouse model was developed and used to test its *in vivo* activity.

Results: Cell lines tested were sensitive to CDK4/6 inhibition, independent on *RB1* gene status. Transcriptome analyses and knockdown experiments revealed a major role for FOXM1 in this response. CDK4/6 inhibition resulted in reduced FOXM1 phosphorylation *in vitro* and *in vivo* and showed synergy with CDDP, allowing a significant tumor regression. FOXM1 exerted important oncogenic roles in bladder cancer.

Conclusions: CDK4/6 inhibitors, alone or in combination, are a novel therapeutic strategy for patients with advanced bladder cancer previously classified as unfit for current treatment options.

Introduction

Bladder cancer is the most common malignancy of the urinary tract (1). At diagnosis, two major classes of bladder cancer are distinguished (2): approximately 75% of patients present a non-muscle–invasive disease (NMIBC, stage Ta, T1 or CIS), while the rest of the patients (25%) show a tumor already invading the muscle layers (MIBC stage T2 or higher). NMIBC is considered a relatively indolent tumor, and treated by transurethral resection (3). In the case of high-risk tumors, this can be followed by intravesical instillation with Bacillus Calmette-Guérin or mitomycin (3). Nevertheless, NMIBC displays one of the highest recurrence rates among all cancers, and a significant part of these recurrences shows tumor progression toward MIBC (4). The treatment of MIBC includes a radical cystectomy usually followed by cisplatin (CDDP)-based chemotherapy (5). Unfortunately, the disease becomes metastatic in a high proportion of the cases (50%–70%), leading to extremely low survival rates (5, 6). This scenario aggravates when considering the elevated mean age of patients at diagnosis, associated to frequent and severe comorbidities in almost 50% of patients with MIBC (6). Such patients, often called "unfit", are not candidates to CDDP treatment having few therapeutic options (6). In spite of multiple trials aimed to develop new therapeutic options for patients with bladder cancer, few improvements have occurred in the last decades with the exception of immune checkpoint inhibitors. In this regard, although these inhibitors have demonstrated promising results in some cases, the proportion of patients who shows objective responses to these therapies is still very limited (20%–35%; refs. 7–9). Consequently, there is an urgent need of new avenues for the management of advanced bladder cancer.

The molecular portrait of bladder cancer has identified multiple alterations that could be actionable through

[1]Biomedical Research Institute, University Hospital "12 de Octubre," Madrid, Spain. [2]Centro de Investigación Biomédica en Red de Cáncer (CIBERONC), Madrid, Spain. [3]Molecular Oncology Unit, CIEMAT, Madrid, Spain. [4]Genomic Instability Group, CNIO, Madrid, Spain. [5]Genetic & Molecular Epidemiology Group, CNIO, Madrid, Spain. [6]Epithelial Carcinogenesis Group, CNIO, Madrid, Spain. [7]Departament de Ciències Experimentals i de la Salut, Universitat Pompeu Fabra, Barcelona, Spain.

Note: Supplementary data for this article are available at Clinical Cancer Research Online (http://clincancerres.aacrjournals.org/).

C. Rubio and M. Martínez-Fernández contributed equally to this article.

Current address for M. Martínez-Fernández: Mobile Genomes and Disease Lab, CIMUS, Universidade de Santiago de Compostela, Barcelona, Spain; current address for F. Villacampa, Urology Department, Clínica Universidad de Navarra, Madrid, Spain; and current address for S. Ruiz, Laboratory of Genome Integrity, NCI, NIH, Bethesda, Maryland.

Corresponding Author: Jesus M. Paramio, Molecular Oncology Unit, CIEMAT, Avd Complutense 40, Madrid E-28040, Spain. Phone: 349-1496-2517; Fax: 349-1346-6484; E-mail: jesusm.paramio@ciemat.es

doi: 10.1158/1078-0432.CCR-18-0685

Translational Relevance

The gold standard in the treatment of advanced bladder cancer remains radical surgery followed by cisplatin-based chemotherapy. However, close to 50% of patients are considered unfit to receive cisplatin, thus reducing treatment options. Here, we describe the preclinical efficacy of CDK4/6 dual inhibitors using a variety of *in vitro* and *in vivo* models. Remarkably, the activity of CDK4/6 dual inhibitor is partially independent on *RB1* gene status and shows dramatic synergistic effect with cisplatin, allowing a significant reduction in the dose of this chemotherapeutic agent. Our data support a potential effect of CDK4/6 dual inhibitor on FOXM1 phosphorylation and activation. Because FOXM1 exerts major roles in bladder cancer, our results support the preclinical rationale for a human trial using these compounds, alone or in combination, for the clinical management of patients with cisplatin-unfit bladder cancer, especially in those cases showing high FOXM1 phosphorylation.

molecularly targeted therapies (10, 11). Among them, the RB pathway is predominantly altered (10, 11). This can result from the inactivation of *RB1* gene itself, or by mutation or amplification of different genes whose products mediate the functional inactivation of the pRb protein (10, 11). On the basis of this, drugs targeting these proteins are attractive therapeutic tools. Among them, CDK4/6 inhibitors are being tested in a large number of solid malignancies characterized by the presence of wt *RB1* alleles and/or cyclin D or *CDK4/6* amplification. In fact, they have been recently approved for treating hormone receptor–positive breast tumors in combination with compounds targeting ER-dependent signaling (12).

Here, we report the preclinical analysis of a CDK4/6 inhibitor in bladder cancer. Our current data show that this inhibitor exerts relevant antitumor effects *in vitro* and *in vivo*, affecting not only *RB1* wt but also *RB1*-mutant tumors. In both cases, we find that such activities also rely on the inhibition of the FOXM1 phosphorylation and activation. In addition, treatment with CDK4/6 inhibitor sensitizes the cells to CDDP allowing a significant reduction in its effective dose with a consequent reduction in side effects. Therefore, these results collectively open a new avenue of possible bladder cancer therapy, especially for CDDP-unfit patients.

Materials and Methods

Cell lines and reagents

The bladder cancer cell lines (RT112, J82, 253J, 5637, UM-UC-1 and RT4), with known genomic characteristics (13) and validated by short tandem repeat typing, were maintained in DMEM GlutaMAX (Gibco-BRL Life Technologies) with 10% FBS (Hyclone) and 1% antibiotic–antimycotic (Gibco-BRL Life Technologies) at 37°C in a humidified atmosphere of 5% CO_2. Palbociclib isethionate (provided by Pfizer through a Compound Transfer Program grant) was dissolved in PBS. CDDP (Selleckchem) was dissolved in PBS (Sigma). Cell viability and cell-cycle assays are described in detail in Supplementary Material and Methods.

Tumor xenografts and transgenic mouse model

All the animal experiments were conducted in compliance with CIEMAT guidelines, and approved by the Animal Welfare Department of the Comunidad de Madrid (Spain; PROEX 088-15, PROEX 183/15). Palbociclib and CDDP concentrations were chosen based on previously published data (14, 15). After 15–30 days of treatment, mice were sacrificed and tumors were collected and processed. The transgenic mice were generated by breeding $Rb1^{F/F}$;$Rbl1^{-/-}$ (16) and $Trp53^{F/F}$;$Pten^{F/F}$ (17) mice. Adenovirus expressing Cre recombinase under keratin K5 promoter (18) was obtained from the Viral Vector Production Unit of the Autónoma University of Barcelona and surgically delivered into the bladder lumen as described previously (19, 20). Tumor appearance was routinely followed by visual inspection, hematuria, and abdominal palpation. At the time of sacrifice, tissues were collected and processed as reported previously (16, 21, 22). To test the effectiveness of CDDP plus palbociclib, tumor-bearing mice were treated for 28 days with vehicle ($n = 20$) or with daily palbociclib plus a once per week dose of CDDP ($n = 20$). Males and females were randomly adjusted to 50% on each group.

Immunoblot and IHC

IHC and immunoblots were performed essentially as described previously (20). Antibodies used are listed in Supplementary Table S1 (more information in Supplementary Material and Methods).

Patient series and clinical data

All studies involving patients were conducted in accordance with the Declaration of Helsinki and the International Conference on Harmonization Good Clinical Practice guidelines. All patients provided written informed consent before study entry. For the University Hospital "12 de Octubre" cohort (Spain), tumor and nontumoral paired samples and medical records were analyzed from 87 patients (pathologic and clinical data are shown in Supplementary Table S2). Informed consent was obtained from all the patients and the study was approved by the Ethical Committee for Clinical Research of University Hospital 12 de Octubre (IRB ref. 10/050; refs. 23, 24). Resources from the EPICURO Study including 832 newly diagnosed urothelial bladder cancer (UBC) cases aged 22–80 years with a median follow-up of 70.7 months (range 0.7–117.7 months), and available tumor tissue were used to replicate previous results on FOXM1-P prognostic value. Informed consent was obtained from study participants in accordance with the Institutional Review Board of the Ethics Committees of participating hospitals that approved the study (IRB Hospital del Mar, ref. 2008/3296/1). More information is provided in Supplementary Materials and Methods.

qRT-PCR

Total RNA was isolated using miRNeasy Mini Kit (Qiagen) according to the manufacturer's instructions and DNA was eliminated (Rnase-Free Dnase Set, Qiagen). Reverse transcription was performed using the Omniscript RT Kit (Qiagen); *TBP* was used as reference gene using 50 ng of total RNA and specific primers (Supplementary Table S3). PCR was performed in a 7500 Fast Real Time PCR System using GoTaq PCR master mix (Promega). Melting curves were performed to verify specificity and absence of primer dimers. Reaction efficiency was calculated for each primer combination.

Gene expression microarray analyses

Control (PBS-treated) and palbociclib-treated (IC_{50}) RT112, J82 and 5637 cells, were analyzed using the GeneChip Human Transcriptome array (HTA) V2 Arrays (Affymetrix). Data are deposited in GEO (GSE105402). In the case of transgenic mouse samples, microdissections of the tumors were carried out before RNA extraction to avoid any possible contamination. Total RNA was extracted using miRNeasy FFPE kit (Qiagen). cDNAs from 12 ng of total RNA were generated, fragmented, biotinylated, and hybridized to the GeneChip Mouse Transcriptome Array 1.0 (MTA 1.0.), now known as Clarion D Assay Mouse (Affymetrix, Thermo Fisher Scientific). Data are deposited in GEO (GSE100716). The protocol followed and the normalization procedures for both datasets are described in the Supplementary Information.

Statistical analyses

Comparisons between groups were made using the Wilcoxon–Mann–Whitney test. Survival analyses (recurrence free or tumor progression in recurrence) according to various variables were performed using the Kaplan–Meier method and statistical differences between the patient groups were tested by the log-rank test. Contingency analyses were made using the Fisher exact test. Tumor growth differences were determined by ANOVA followed by Bonferroni multiple comparison tests. Significance of correlations was determined by Spearman rank order test. Discrimination between samples showing increased or decreased tumor/normal relative expression of either gene or miRNA expression was made using the median. SPSS 17.0 and GraphPad Prism 6.0 software were used.

Results

CDK4/6 inhibitor is active in bladder cancer cells regardless of their *RB1* gene status

Six different bladder cancer cell lines of known genomic characteristics [5637 and J82 (*RB1* mutant) and RT112, 253J, UM-UC-1 and RT4 (*RB1* wt)], and representative of various tumor stages and bladder cancer subtypes (13), displayed a similar sensitivity to CDK4/6 inhibitor in a range of concentrations similar to those reported for other tumor cells (ref. 25; Supplementary Fig. S1). We observed no significant differences in their IC_{50} values depending on the *RB1* status by XTT analyses (Fig. 1A). These findings were also supported by the analysis of the Cancer Cell line Encyclopedia collection (https://portals.broadinstitute.org/ccle) on urothelial cells or in small-cell lung cancer (SCLC, where *RB1* mutations are prominent; Supplementary Fig. S2). We also observed that treated cells presented differences in their cell-cycle profiles: while *RB1* wt cells had a marked reduction in the percentage of S-phase entry with cells arresting in G_1, *RB1*-mutant cells displayed a prominent reduction of G_2–M phase entry and a significant induction of apoptosis (sub-G_1 cells; Fig. 1B). Immunoblot studies showed that palbociclib caused inhibition of pRb phosphorylation in *RB1* wt cells (Fig. 1C). In contrast, in *RB1*-mutant cells, besides the expected pRb absence, a reduction of Cyclin B and E2F3a expression was found (Fig. 1C). Finally, p27 induction was detected in all cells regardless their *RB1* status (Fig. 1C). Tumor xenograft experiments revealed that CDK4/6 inhibition exerts similar activities *in vivo*, independently of *RB1* status (Fig. 1D). IHC analyses showed a reduction of Ki67 in *RB1* wt cell–derived tumors (Supplementary Fig. S3), in agreement with the *in vitro* cell-cycle profile data (Fig. 1B), whereas the decrease of phosphorylated histone H3 (pH3, indicative of mitosis) was more evident in *RB1*-mutant cell-derived tumors (Supplementary Fig. S3). Apoptosis, monitored by active caspase-3 expression (Supplementary Fig. S3), was only induced in *RB1*-mutant cell-derived tumors. As expected, the inhibition of pRb phosphorylation was only observed in tumors derived from *RB1* wt cells (Supplementary Fig. S3).

Inhibition of FOXM1 phosphorylation by CDK4/6 inhibitor

To analyze the possible mechanism underlying the above described results, whole-transcriptome analyses were performed in RT112 (*RB1* wt), J82 and 5637 (*RB1* mutant) cells, upon treatment with palbociclib, finding prominent gene expression changes (Fig. 2A; Supplementary Table S4). A poor overlap of up- and downregulated genes was found among the three lines (Fig. 2B). In accordance, Gene Ontology analyses revealed few common functions affected by CDK4/6 inhibition (Supplementary Fig. S4). The putative binding motif enrichment from ChIP-Seq databases using Enrichr webtool (26) also revealed disparities among the deregulated genes in *RB1* wt versus mutant cells (Supplementary Fig. S4). Interestingly, a significant fraction of the downregulated transcripts in both *RB1* wt and *RB1* mut cells showed binding sites for FOXM1 transcription factor (Fig. 2C), whereas those bound by E2F proteins appeared more significantly involved in *RB1* wt cells (Fig. 2C). As CDK4 activates FOXM1 through phosphorylation in various residues including Thr600 (27), we analyzed the expression of the phosphorylated Thr600-FOXM1 in parallel with other oncogenic kinases upon palbociclib treatment (27). We observed a significant reduction of phosphorylated Thr600-FOXM1 in all cells, without significant changes in phospho-AKT, phospho-ERK1/2, or total FOXM1 levels (Fig. 2D). To validate this finding *in vivo*, we analyzed the expression of phosphorylated Thr600-FOXM1 in the xenografts derived from *RB1* wt and mutant cells. In both cases, a significant inhibition was observed as a consequence of CDK4 inhibitor treatment *in vivo* (Fig. 2E). This was further supported by the reduction of phosphorylated Thr600-FOXM1 levels upon CDK4 knockdown (Fig. 2F) in RT112 and 5637 cells. On the other hand, CDK2 knockdown increased FOXM1 and phosphorylated Thr600-FOXM1 in RT112 (Fig. 2F′), whereas the moderate decrease in CDK2 levels decreased the phosphorylated Thr600-FOXM1 in 5637 cells (Fig. 2F′).

To analyze whether sensitivity to CDK4/6 inhibitor is dependent on FOXM1, we performed transfection experiments. We found that increased levels of FOXM1, which were accompanied with its increased phosphorylation, conferred higher sensitivity to CDK4/6 inhibitor, whereas the reduction of FOXM1 promoted resistance only in *RB1*-mutant cells (Supplementary Fig. S5). This is in line with FOXM1 as potential surrogate target of CDK4/6 inhibition, as the reduction or increased levels of a certain target may define resistance or sensitivity, respectively, to determined antitumor compound. In support of this, the levels of *FOXM1* mRNA inversely correlated with sensitivity to palbociclib in *RB1*-mutant bladder cancer and SCLC (Supplementary Fig. S6). These results indicate that, in the absence of mutations, pRb is a primary determinant of palbociclib sensitivity. Then, we decided to determine whether reduction of FOXM1 could affect tumor growth *in vivo*. Xenograft experiments using parental or FOXM1-knockdown-RT112 (*RB1* wt) and FOXM1-knockdown-5637 cells (*RB1* mut) confirmed a significant inhibition of tumor growth as

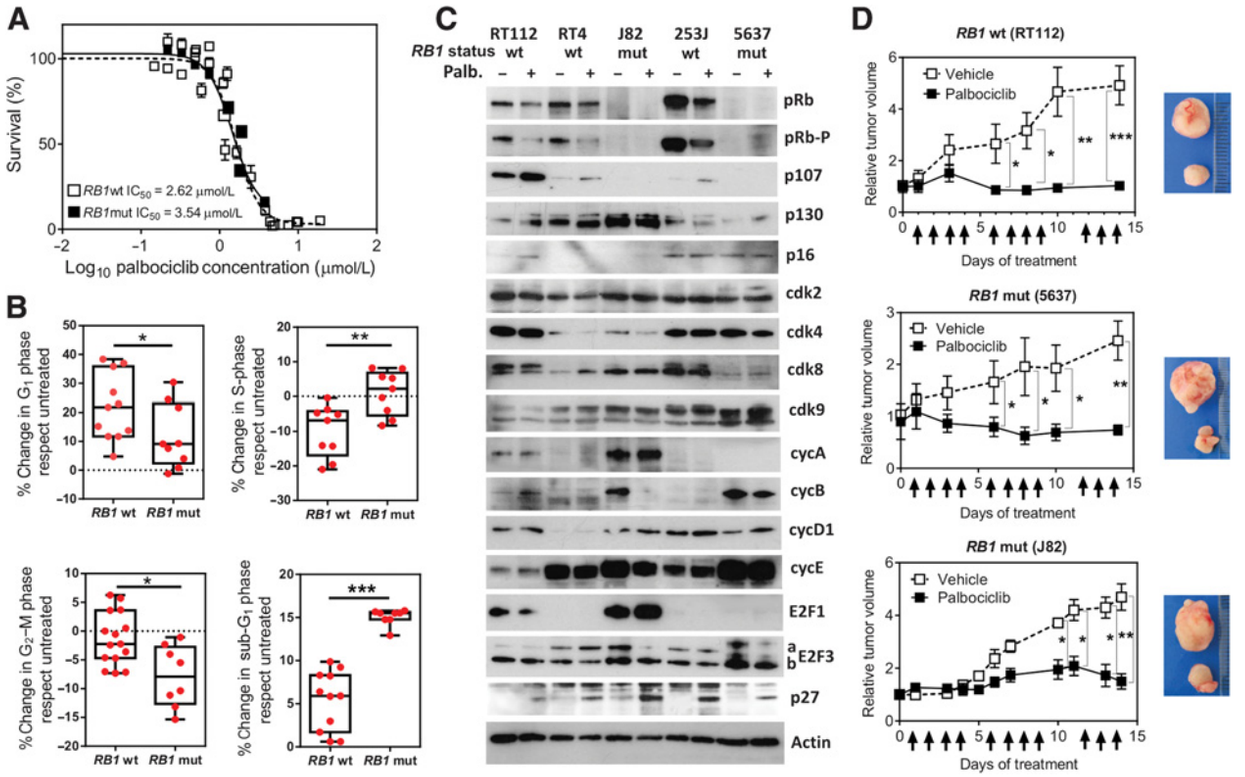

Figure 1.

Palbociclib is active in bladder cancer cell lines irrespective of the *RB1* gene status. **A,** Summary of sensitivity assays using XTT (see Supplementary Fig. S1) of bladder cancer cell lines grouped according *RB1* gene status. Data come from five independent experiments for each cell line relative to untreated cells and afterwards grouped according to the *RB1* gene status and shown as mean ± SEM. **B,** Summary of cell-cycle changes as a consequence of palbociclib treatment. Cells were treated for 24 hours in the presence of palbociclib (at the IC_{50} dose) and cell-cycle profiles were analyzed by flow cytometry. Data come from 5–10 independent experiments (shown in red) for each cell line relative to untreated cells and afterwards grouped according the *RB1* gene status and shown as box plots (95% confidence interval) and mean ± SEM. **C,** Immunoblot of the quoted proteins in the untreated and palbociclib-treated (IC_{50} for 24 hours) different cell lines. Actin was used to normalize loading. The status of *RB1* gene is shown for each cell line (detailed representative mutations of each cell line are provided in Supplementary Fig. S1). **D,** Summary of palbociclib effects on tumor growth from RT112-, 5637-, and J82-derived xenografts. Arrows denote the time points of palbociclib administration. Inset panels show examples of untreated (above) and treated (below) tumors at the end of the experiment for each cell line (*, $P \leq 0.05$; **, $P \leq 0.01$; ***, $P \leq 0.005$).

consequence of FOXM1 level reduction (Supplementary Fig. S5). Of note, we observed that the knockdown of FOXM1 induced features of senescence in *RB*1 wt cells, whereas it also promoted massive apoptosis in *RB*1-mutant cells (Supplementary Fig. S5), which is in agreement with the observations upon palbociclib treatment (Fig. 1 and data not shown).

Synergy between CDK4/6 inhibitor and CDDP

On the basis of recent data indicating that increased expression or activity of FOXM1 can confer platinum resistance (28), we decided to check whether CDK4/6 inhibition may affect the response to CDDP. We performed sensitivity curves of CDDP alone or in the presence of palbociclib. A dramatic increase in CDDP sensitivity was observed in all palbociclib-treated cell lines (Supplementary Fig. S7). In fact, cooperativity studies using the Chou–Talalay method (29) showed a systematic synergy between CDDP and palbociclib, as demonstrated by the combination index < 1 in all cell lines (Fig. 3A). Importantly, the overexpression or knockdown of FOXM1 produced increased resistance or sensitivity to CDDP in RT112 and 5637 cells, respectively (Supplementary Fig. S8A). On the other hand, the knockdown of CDK4 had no effect on CDDP sensitivity, whereas it conferred resistance to palbociclib (Supplementary Fig. S8B). Given that the reduction of CDK4 levels accounted for decreased FOXM1 and phosphorylated FOXM1 levels (Fig. 2), these results suggest that the absence of CDK4, but not the inhibition of its kinase activity, might induce a FOXM1-independent mechanism that allows retaining CDDP sensitivity.

We next studied whether the synergy between CDDP and palbociclib could be affected by different FOXM1 levels. Therefore, we performed cooperative analyses using RT112 or 5637 cells upon overexpression or knockdown of FOXM1. The results (Supplementary Fig. S9) indicated that the synergy between palbociclib and CDDP is maintained irrespective of FOXM1 altered expression in 5637 cells, whereas the knockdown of FOXM1 accounted only for additive effect in RT112 cell line. These results can be explained by the altered independent sensitivity to CDDP or palbociclib promoted by alterations in FOXM1 levels, suggesting that increased resistance to CDDP promoted by increased expression of FOXM1 is counteracted by the increased

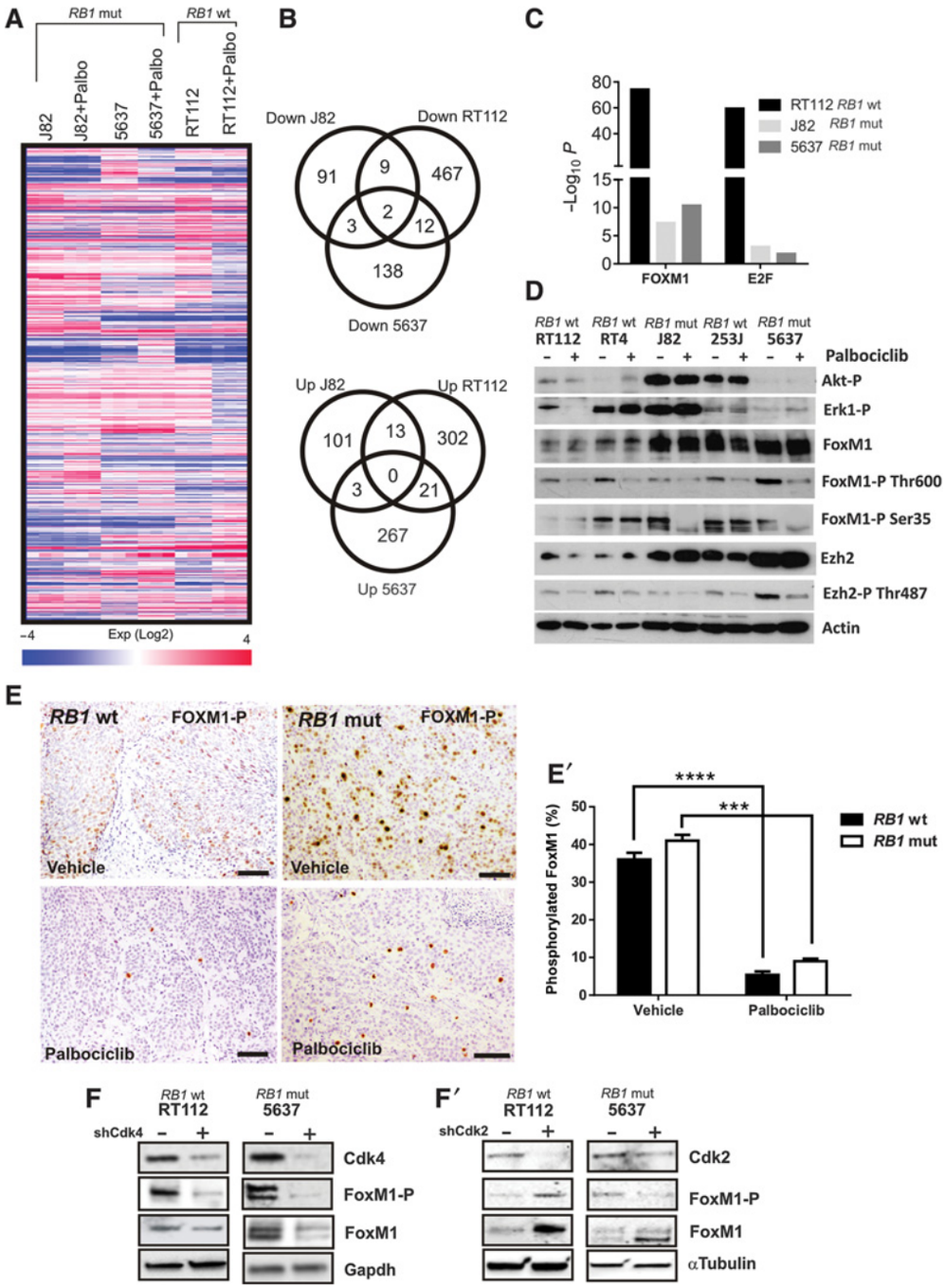

Figure 2.

Identification of FOXM1 as a putative effector of palbociclib in bladder cancer cells. **A,** Heatmap showing global transcriptome changes in J82, 5637, and RT112 cells as a consequence of palbociclib (Palbo) treatment (IC_{50} dose for 24 hours). **B,** Venn diagrams showing the overlapping of transcripts downregulated (top) or upregulated (bottom) in the different cells lines as a consequence of palbociclib treatment. **C,** Summary of putative binding motif enrichment analysis using the Enrichr webtool (26, 55), showing the relative relevance of FOXM1 or E2F transcription factors as transcriptional activators of the downregulated transcripts. **D,** Immunoblot of the quoted proteins in the untreated and palbociclib treated (IC_{50} for 24 hours) different cell lines. Actin was used to normalize the loading. **E,** Examples of control and palbociclib-treated tumor xenografts from RT112 (*RB1* wt) and 5637 (*RB1* mut) stained against FOXM1-Thr600-P (FOXM1-P). Scale bars, 150 μm. **E′,** Summary of the quantitative analyses of FOXM1-P staining. Data come from five different tumors for each cell line and condition (three independent slides) and are shown as mean ± SEM. ****, $P \leq 0.0001$; ***, $P \leq 0.0005$ determined by the Mann–Whitney test. **F**, **F′,** Immunoblot of RT112 and 5637 cells upon knockdown of CDK4 (**F**) or CDK2 (**F′**) showing that the reduction of CDK4 levels is accompanied by a reduction in FOXM1 phosphorylation (Thr600) in RT112 and 5637 cells, whereas CDK2 knockdown produced increased expression of FOXM1 and phosphorylated FOXM1 in RT112 cells (**F′**).

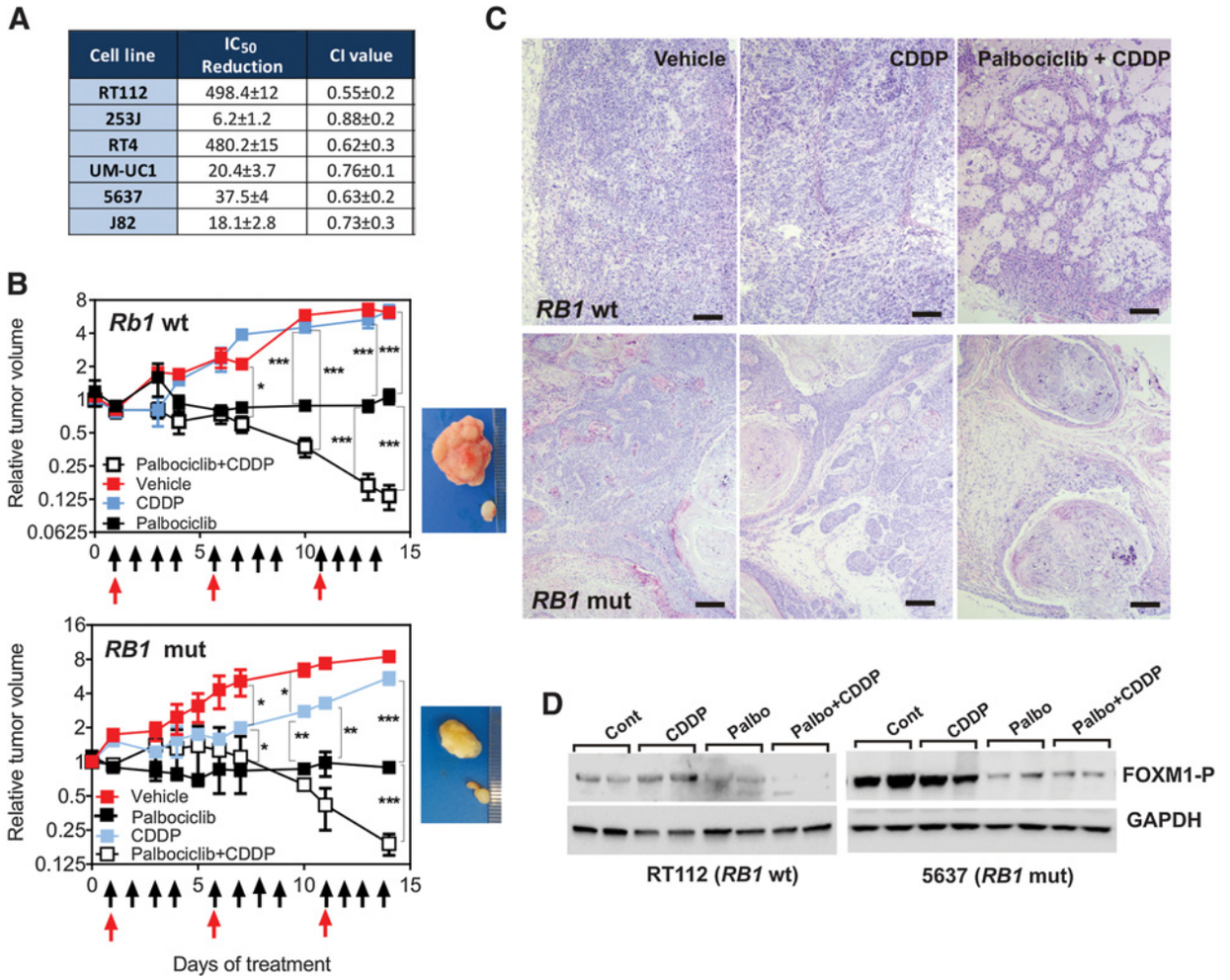

Figure 3.

Palbociclib synergizes with CDDP in bladder cancer cell lines. **A,** Summary of CDDP increased sensitivity (see Supplementary Fig. S5) of bladder cancer cell lines as a consequence of treatment with palbociclib. Data show the fold change reduction of CDDP IC_{50} and the combination index (CI) using the Chou–Talalay method (29). Data come from 5 to 10 independent experiments. **B,** Summary of CDDP and palbociclib + CDDP effects on tumor growth from RT112 (top *RB1* wt) and 5637 (bottom *RB1* mut) derived xenografts. Black arrows denote the time points of palbociclib administration; red arrows denote the CDDP administration. Inset panels show examples of untreated (above) and treated (below) tumors at the end of the experiment for each cell line and data are expressed as mean ± SEM. *, $P \leq 0.05$; **, $P \leq 0.01$; ***, $P \leq 0.005$; ****, $P \leq 0.001$ as determined by Bonferroni two-way ANOVA multiple comparisons. **C,** Representative histology of tumor xenograft from RT112 (top, *RB1* wt) and 5637 cells (bottom, *RB1* mut) derived xenografts in controls (vehicle treated) or upon CDDP or palbociclib + CDDP treatment. Scale bars, 250 μm. **D,** Immunoblot of the tumor xenografts from RT112 and 5637 cells showing the reduction in FOXM1 phosphorylation (Thr600) as consequence of the different treatments (see also Fig. 1D). GAPDH was used to normalize loading.

sensitivity to palbociclib in RB wt and RB-mutant cells. On the other hand, in Rb wt, but not in Rb-mutant cells, the reduced FOXM1 levels accounted for a minor effect probably because the sensitivity to palbociclib is predominantly dictated by pRb phosphorylation in these cells (see also Supplementary Fig. S2A).

To confirm the synergy between palbociclib and CDDP shown *in vitro*, we treated xenografts from RT112 and 5637 cells with palbociclib, CDDP, or CDDP plus palbociclib finding that, while treatment with CDDP had no significant effects on tumor growth (Fig. 3B; Supplementary Fig. S9), the combined treatment produced a dramatic reduction on tumor growth (Fig. 3B), and in most cases evident tumor regression (Supplementary Fig. S10A and S10A′), both in *RB1* wt and *RB1*-mutant cell-derived tumors (Fig. 3B). The histology of these tumors also showed a severe reduction in cellularity upon the combined treatment (Fig. 3C). Immunoblots revealed a significant reduction in phosphorylated FOXM1 in the tumors derived from both cell lines after palbociclib or palbociclib + CDDP treatments (Fig. 3D). IHC studies not only supported this FOXM1 phosphorylation reduction, but also demonstrated a substantial inhibition of proliferation and a large induction of apoptosis as a consequence of the combined treatment (Supplementary Fig. S10).

Effectiveness of palbociclib plus CDDP in a mouse model of metastatic bladder cancer

To explore whether palbociclib can be active in bladder cancer in a more physiologic *in vivo* context, we generated a novel metastatic bladder cancer transgenic mouse model. We used a

previously validated model of invasive bladder cancer in which *Pten* and *Trp53* tumor suppressor gene loss is induced by instillation of adenoviruses coding for Cre recombinase (19). To selectively induce recombination in urothelial epithelial cells, we replaced the general CMV promoter by the regulatory elements of keratin K5 (AdK5Cre). This drives the expression of the recombinase exclusively to basal urothelial cells as assessed by ROSA26 reporter analyses (not shown). In addition, we introduced $Rb1^{F/F}$; $Rbl1^{-/-}$ alleles to induce Rb deficiency, and to circumvent possible compensatory mechanisms (30), obtaining quadruple knockout mice (QKO): $Pten^{F/F}$; $Trp53^{F/F}$; $Rb1^{F/F}$; $Rbl1^{-/-}$. After 90–120 days of the intravesical AdK5Cre inoculation, all the mice presented tumor lesions (Fig. 4A), characterized as highly aggressive urothelial tumors that invaded the muscle layer (Fig. 4B) and surrounding organs, even developing metastasis to the lungs (Fig. 4C), liver (not shown), and peritoneal cavity (Fig. 4C′).

The whole transcriptome (Supplementary Table S5) characterization of the primary tumors and their metastases compared with control bladder (siblings noninoculated with AdK5Cre) by Gene Set Enrichment Analysis (GSEA; ref. 31) displayed an increased expression of E2F and MYC target genes, induction of epithelial–mesenchymal transition, angiogenesis, and IFNγ response genes, as well as a decreased expression of Hedgehog signaling genes (Supplementary Fig. S11A). Moreover, analyses using Enrich web tool revealed upregulated cell cycle, DNA repair/replication, and chromatin-remodeling genes, primarily bound by E2F, MYC, and, remarkably, FOXM1 (Supplementary Fig. S11B, S11C′, and S11D′). The downregulated genes in these analyses were primarily involved in muscle organization (according to the invasive behavior of tumor cells reducing muscle component), VEGF signaling, negative regulation of intracellular signaling, and extracellular matrix organization (Supplementary Fig. S11B and S11C), and presented binding to various transcriptional regulators including Polycomb members (Supplementary Fig. S11D), which is in agreement with previous findings of the oncogenic activities of these chromatin-remodeling processes in bladder cancer (reviewed in ref. 32). Finally, we observed a significant overlap of the genes upregulated and downregulated with various series of infiltrating human bladder cancer datasets (Oncomine database), also with poor clinical outcome and *RB1* mutation (Supplementary Table S6).

Given the characteristics of the mouse model and its similarities with advanced human bladder cancer samples, we decided to explore the effectiveness of the palbociclib plus CDDP combined treatment. We observed a significantly increased survival in the palbociclib + CDDP cohort (Fig. 4A). Necropsies showed the presence of bladder tumors (Fig. 4B, B′) and metastasis (Fig. 4C, C′, and D). However, whereas in the control group, all mice displayed aggressive invasive tumors as commented above (Fig. 4B), in the treatment group a large fraction of the animals showed only tumor remnants with reduced invasion of the surrounding muscle layer (Fig. 4B′), and a severely decreased metastatic burden (Fig. 4A). In the treated group, we further observed clear signs of tumor regression (Supplementary Fig. S12) with necrotic areas and massive lymphocyte infiltrates, which also affected the metastases (Fig. 4D; Supplementary Fig. S12). IHC studies revealed significant inhibition of proliferation, as demonstrated by the impaired BrdUrd incorporation and reduced pH3 (Fig. 4E and F), accompanied by apoptosis induction (Fig. 4G). Similar analyses also showed a significant inhibition of FOXM1 phosphorylation (Fig. 4H and M). There were no major effects on AKT, STAT3, or ERK activation in the treated tumors (Fig. 4I, J, K, and M). In contrast, the expression of EZH2 was reduced (Fig. 4L and M).

In the genomic characterization of these QKOs, unsupervised analysis showed that treated tumors clustered with control bladder samples. We also observed strong transcriptional changes as a consequence of the treatment (Fig. 4N). GSEA analyses revealed a reduced activation of E2F and MYC target genes in the treated tumors (Supplementary Fig. S13), along with G_2–M checkpoint and genes induced by VEGF (Supplementary Fig. S13). Moreover, we observed inhibition of K-Ras–dependent genes in treated tumors (Supplementary Fig. S13) and increased xenobiotic genes, according to the expected metabolism of antitumor drugs (Supplementary Fig. S13). Although no significant involvement of transcriptional regulators or gene ontologies were found in the case of upregulated transcripts, a preferential regulation by FOXM1 and E2F transcription factor was detected for the downregulated genes, along with reduced histone marks associated with transcriptional activation (Fig. 4O). These downregulated transcripts were primarily involved in cell cycle, telomere maintenance, chromosome organization, and DNA repair (Fig. 4P). Moreover, they presented a statistically significant overlap with the genes displaying reduced expression in a variety of human cancer cell lines upon treatment with palbociclib (Fig. 4Q).

Relevance of FOXM1 in human bladder cancer

The above results prompted us to analyze the possible relevance of FOXM1 in human bladder cancer. First, we studied gene expression data from a previous NMIBC-enriched patient series (Supplementary Table S2; ref. 23). The upregulated genes in primary tumors displaying recurrences (Fig. 5A) were typified by the binding of FOXM1, E2F, and MYC (Fig. 5B). They also displayed a significant overlap with those genes downregulated by palbociclib treatment on multiple cell lines representative of different cancer types (Fig. 5C). Remarkably, when samples were classified in an unsupervised manner according to the expression of FOXM1-bound genes (33, 34), a clear discrimination between normal and tumor samples was found and it discriminated those primary tumors corresponding to patients that suffered disease recurrence (Fig. 5D). The expression of the *FOXM1* gene, in larger series analyzed by qRT-PCR, confirmed an increased expression in tumor tissues (Fig. 5E). Among tumors, increased *FOXM1* expression was found in high-grade samples (Fig. 5G) and in those tumors of patients showing recurrence (Fig. 5H) or progression in recurrence (Fig. 5I). However, no differences were found between low-stage tumors (Ta–T1; Fig. 5F). By IHC (23), we observed that the expression of phosphorylated Thr600-FOXM1–discriminated tumors from patients showing early recurrence (Fig. 5J and K).

To further support these findings, we used a large epidemiologic series of primary bladder cancer encompassing the full spectrum of the disease (EPICURO study; ref. 35). The expression of phosphorylated Thr600-FOXM1 was found to be significantly higher in high-stage and high-grade tumors (Supplementary Table S7). Moreover, patients whose tumors showed high p-FOXM1 expression had a lower progression-free survival, although the disease-specific survival (DSS) was not statistically significantly different (Supplementary Table S8). In multivariate analysis adjusted for age, gender, stage, and grade, we also observed (Supplementary Table S7) that high p-FOXM1 was significantly associated with a higher risk of progression. In the stratified analysis by risk groups, the increase in risk of progression

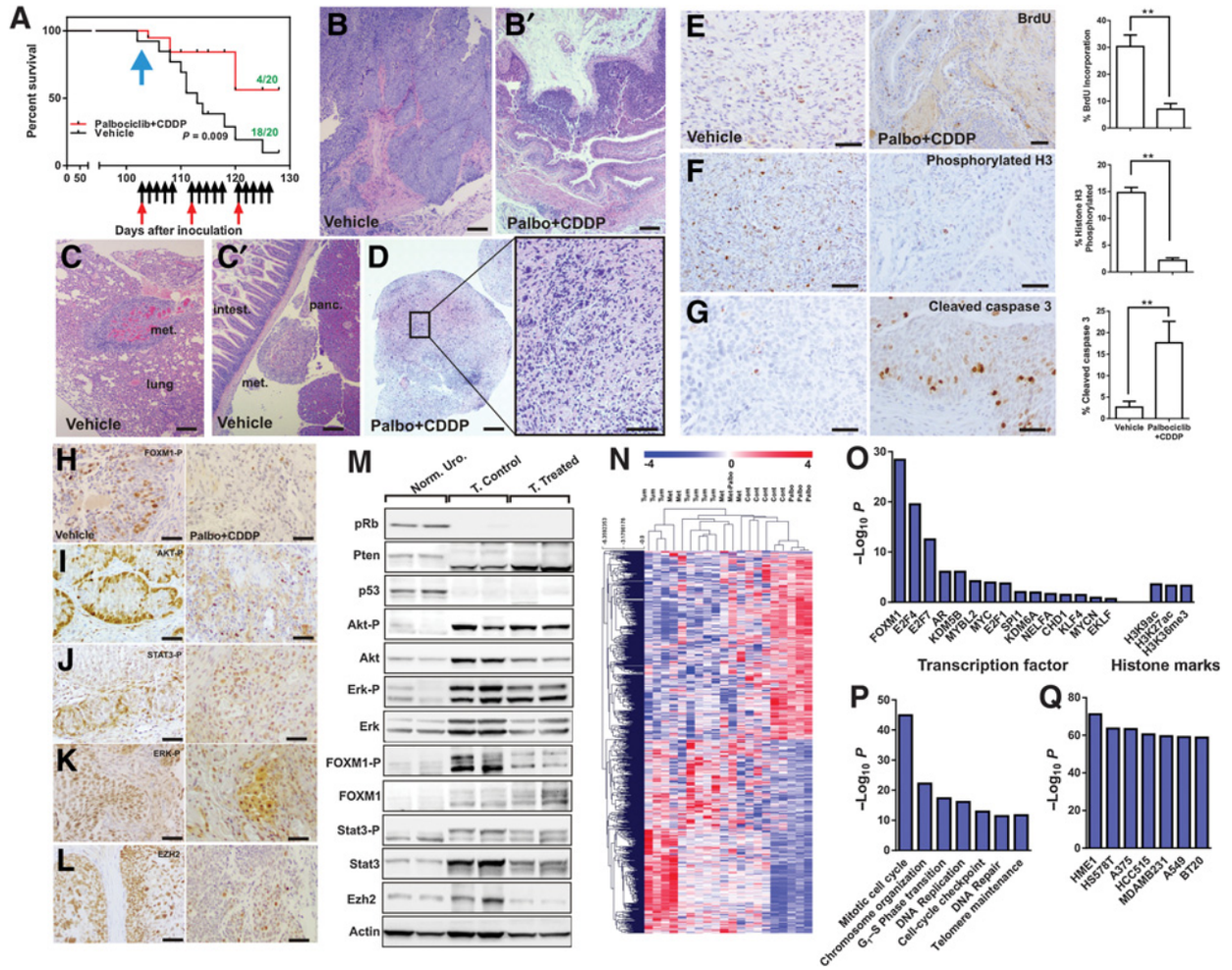

Figure 4.

Effectiveness of palbociclib plus CDDP treatment in a metastatic bladder cancer mouse model. **A,** Kaplan–Meier curve displaying survival in the treated and control cohorts ($n = 20$ on each). *P* value was obtained using the log-rank test. Arrow denotes the treatment start. Numbers indicate the mice showing metastases in each cohort. **B–D,** Representative histology examples of bladder tumor (**B**, **B′**) and lung (**C**) and visceral (**C′**, **D**) metastasis in vehicle (**B**, **C**, **C′**) and in palbociclib + CDDP–treated mice (**D**). Note the low infiltrative characteristic of palbociclib + CDDP-treated tumor (**B′**) compared with vehicle-treated tumor (**B**). Inset in **D** shows the high lymphocyte infiltration in a visceral metastasis from a palbociclib + CDDP–treated mouse. Scale bars = 250 μm. **E–G,** Analyses of proliferation measured by BrdUrd incorporation (**E**), histone H3 phosphorylation (**F**), and apoptosis analyzed by cleaved caspase-3 expression (**G**). Left, representative IHC examples of vehicle-treated samples; middle panels, representative IHC examples of palbociclib + CDDP–treated mice; right, quantitative summary of IHC analyses, from at least three independent analyses scoring at least 5 fields per sample, shown as mean ± SEM. **, $P \leq 0.01$ determined by the Mann–Whitney *U* test. Scale bars, 150 μm. **H–L,** Representative IHC images of vehicle (left) and palbociclib + CDDP–treated mouse bladder tumors showing the reduction in phosphorylated FOXM1 (**H**) but not in phosphorylated AKT (**I**), STAT3 (**J**), or ERK (**K**) as a consequence of the treatment. **L,** The expression of EZH2 that is severely reduced in palbociclib + CDDP–treated mouse bladder samples. Scale bars, 150 μm. **M,** Immunoblot analyses of normal urothelium, vehicle, and palbociclib + CDDP–treated mouse bladder tumor samples showing the expression of the quoted proteins. All proteins were normalized using β-actin signal. **N,** Heatmap showing global transcriptome changes in control bladder (Cont), vehicle-treated (Tum), metastasis in vehicle (Met), palbociclib + CDDP (Palbo) metastasis in palbociclib + CDDP (Met-Palbo)–treated mouse bladder tumor samples. **O,** Summary of putative binding motif enrichment analysis using the Enrich webtool (http://amp.pharm.mssm.edu/Enrichr/; refs. 26, 55), showing the relative relevance of various transcription factors and histone marks in the downregulated transcripts in palbociclib + CDDP–treated mouse bladder tumor samples. **P,** Summary of Gene Ontology of biological processes showing the relevant functions of the downregulated genes in palbociclib + CDDP–treated mouse bladder tumor samples. **Q,** Summary of the overlap between the downregulated genes in palbociclib + CDDP–treated mouse bladder samples and genes previously identified as downregulated in the quoted cancer cell lines by palbociclib treatment.

and DSS was restricted to the low-risk NMIBC (HR = 3.9; 95% CI, 1.6–9.31 and HR = 3.1; 95% CI, 0.9–9.6, respectively). In contrast, no differences in risk of progression and DSS were seen in patients with high-risk NMIBC and MIBC, suggesting that additional mechanisms may contribute to tumor aggressiveness in these disease groups.

We next used The Cancer Genome Atlas (TCGA) database, which is composed exclusively of MIBC (10). We found that high *FOXM1* transcript levels were highly significantly associated with shorter disease-specific survival (Fig. 5L). Finally, we analyzed whether different TCGA bladder cancer subtypes displayed increased activity of FOXM1 through GSEA of those

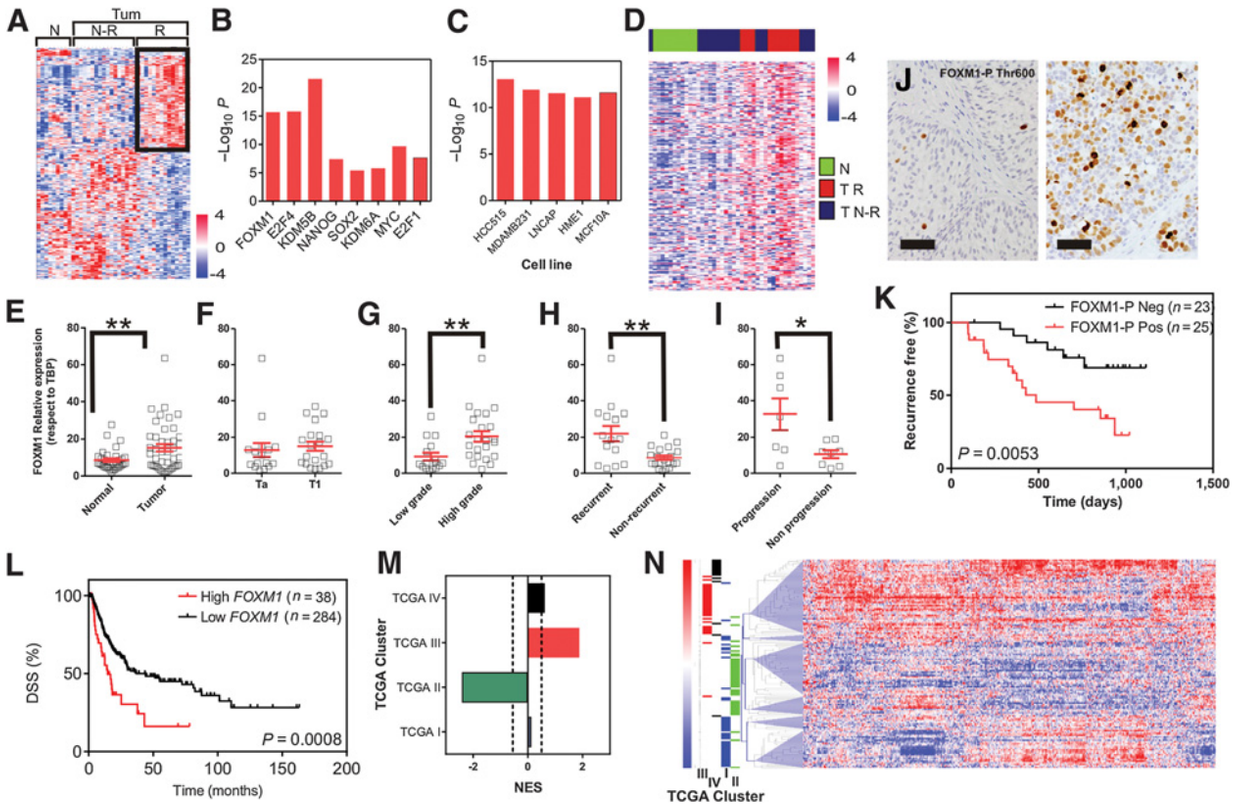

Figure 5.

Relevance of FOXM1 in human bladder cancer. **A,** Heatmap showing the supervised classification of genes discriminating normal (N) and primary tumor samples (Tum) that afterwards displayed recurrence (R) or not (N-R; see ref. 20). **B,** Summary of putative binding motif enrichment analysis in the upregulated genes characteristic of primary tumors that showed recurrence. **C,** Overlap between genes upregulated in primary tumors that showed recurrence and downregulated in the quoted cancer cell lines upon treatment with palbociclib. **D,** Heatmap showing the unsupervised classification of NMIBC patient series according the expression level of genes previously identified as bound and regulated by FOXM1 (34, 56). N denotes normal bladder; T R primary tumor that displayed recurrence during follow up; T N-R primary tumor that displayed no recurrence during follow-up. **E–I,** Summary of qRT-PCR analyses showing *FOXM1* levels in normal and primary tumor samples (**E**), Ta versus T1 stage tumors (**F**), low versus high-grade tumors (**G**), recurrent versus nonrecurrent tumors (**H**) and tumors showing no progression versus tumor showing progression in recurrence (**I**) from NMIBC patient series. *, $P \leq 0.05$; **, $P \leq 0.01$ determined by the Mann–Whitney *U* test. **J,** Representative IHC images of Thr600 phosphorylated FOXM1 expression in NMIBC samples showing a negative (left) and a positive (right) example. Scale bar, 150 μm. **K,** Kaplan–Meier graph showing the recurrence according the negative or positive FOXM1-P expression in human NMIBC samples. *P* value was determined by the log-rank test. **L,** Kaplan–Meier graph showing the DSS of human invasive bladder cancer patients (from TCGA database; ref. 10) according the high or low *FOXM1* gene expression. *P* value was determined by the log-rank test. **M,** Normalized enriched score distribution of genes bound by FOXM1 along the different TCGA bladder cancer subtypes. **N,** Heatmap showing the supervised classification of genes bound by FOXM1 along the different TCGA bladder cancer subtypes.

genes previously identified as FOXM1 targets by ChIP-seq (33, 34). This analysis revealed that TCGA groups III and IV displayed a significant positive enrichment, whereas group II showed negative enrichment (Fig. 5M). This observation was further supported by a supervised classification of TCGA subgroups by the expression of these same genes, showing increased expression in subgroups III and IV, and decreased expression in subgroup II (Fig. 5N). Finally, we monitored possible regulatory mechanisms between *RB1*, *CDK4*, and *FOXM1* in bladder cancer. Using TCGA data, we found that upregulation of *CDK4* and *CDK6* mRNA tended to cooccur with the upregulation of *FOXM1*, which in turn was mutually exclusive with the upregulation of *RB1* (Supplementary Fig. S14A). Overall, altered expression of these genes was associated with reduced DSS (Supplementary Fig. S14B). Similarly, using proteomic data from TCGA, we observed a significant negative correlation between FOXM1 and CyclinD1 or RB protein expression (Supplementary Fig. S14C), whereas no significant correlation was observed between FOXM1 and phosphorylated RB1 (Supplementary Fig. S14C).

Our analyses indicated a possible inverse regulation between RB and FOXM1. In agreement, the knockdown of *RB1* gene in RT112 cells produced a significant increase in FOXM1 expression accompanied with increased CDK4 and Cyclin D3, and decreased Cyclin D1 (Fig. 6A). Because these changes were parallel to increased phosphorylated FOXM1 (Fig. 6A), these observations suggest that activation of FOXM1 might rely on CDK4/6/Cyclin D3 complexes in these cells. Remarkably, the sensitivity to palbociclib is not significantly affected in these cells by the reduction of Rb levels (Fig. 6B), which is in concordance with our above mentioned data.

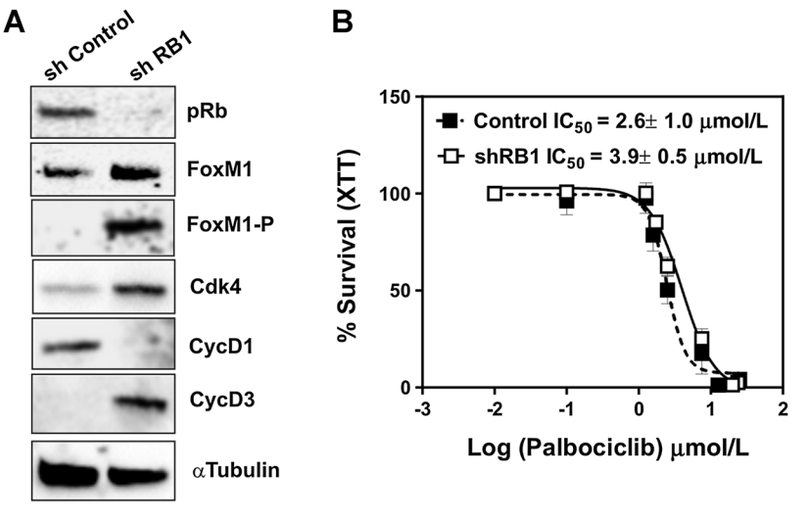

Figure 6.
Interplay between RB pathway and FOXM1 in bladder cancer cells. **A,** Immunoblot showing that the knockdown of RB1 in RT112 cells is accompanied with increased expression of FOXM1, phosphorylated FOXM1, CDK4 and Cyclin D3 and decreased expression of Cyclin D1. Tubulin α was used for loading normalization. **B,** Summary of sensitivity assays of RT112 bladder cancer cells to palbociclib upon knockdown of *RB1*. Data come from eight independent experiments for each cell line derivative (control scrambled shRNA-infected or RB1-silenced cells) and shown as mean ± SEM for each concentration of palbociclib.

Discussion

Bladder cancer represents an important problem for society and health systems due to its increased incidence and prevalence. Moreover, it primarily affects elderly people with very limited therapeutic options. Immune checkpoint inhibitors are the only major improvements since the 1970s, but only a reduced percentage (20%–35%) of patients display objective benefit. In addition, although CDDP-based chemotherapy is effective in advanced bladder carcinoma, the improvement of DSS of these patients is of marginal relevance, as most patients with metastases die from the disease. Here, we present data supporting the basis for a novel approach to treat advanced bladder cancer: palbociclib, a CDK4/6 inhibitor, holds promise as a therapy in bladder cancer.

The rationale for using CDK4/6 inhibitors in the management of solid tumors has been usually associated with a wt *RB1* gene status (12). Accordingly, the common functional inactivation of pRb, which resides in the activity of cyclin D–CDK4/6 complexes, is abrogated by the inhibitor leading to the proliferation arrest. CDK4/6 inhibitors have also gained clinical relevance because they can synergize with other targeted compounds, even being able of overcoming resistance to such treatments (36). Our results indicate that CDK4/6 inhibitor is active (*in vitro* and *in vivo*) in bladder cancer cells regardless their *RB1* status, although the effects on expression of cell-cycle components and dynamics were different in *RB1* wt and mutant cells. In this way, while *RB1* wt cells displayed a predominant cell-cycle arrest in G1, *RB1*-mutant cells showed a reduced entry into G_2–M. To our knowledge, there are few examples of palbociclib antitumor effects regardless of *RB1* status. For instance, in ovarian cancer cells, palbociclib exerts antiproliferative effects irrespective of *RB1* status and cooperates with paclitaxel to induce cell death (37). In the case of *RB1*-mutated hepatoma cells, the sensitivity to palbociclib is due to the upregulation of the pRb relative p107 (38). This compensation has been previously reported regarding acute loss of Rb-related functions (30, 39). However, our analyses revealed no significant induction of p107 (*RBL1*) in *RB1*-mutated bladder cancer cells, while moderate induction of p130 (*RBL2*) was detected without significant changes in p16 (Fig. 1). Moreover, upon palbociclib treatment, we observed induced expression of p107 only in *RB1* wt cells, indicating a different mechanism of action in *RB1* wt versus mutant cells.

In addition to inducing proliferative arrest, palbociclib led to the death of *RB1*-mutant bladder cancer cells. This observation is in agreement with published reports showing that inhibition of cell-cycle kinases or downregulation of cyclins can trigger tumor cell apoptosis, in addition to cell-cycle arrest. Recently, Wang and colleagues have demonstrated that the inhibition of cyclin D3/CDK6 complex by palbociclib also promotes apoptosis irrespective of Rb family status in T-ALL cells (40). Interestingly, this seems to proceed through metabolic reprograming, driving glycolytic intermediates to the pentose phosphate and serine pathways (40). Whether similar changes occur in bladder cancer cells and how this might be affected by functional *RB1* remains unknown. Curiously, our GSEA analyses unveiled metabolic datasets that are altered in transgenic tumors upon palbociclib + CDDP treatment (not shown). Therefore, the possibility that metabolic rewiring also participates in the therapeutic response observed is very attractive and will be subject of future research.

Although the analysis of genes regulated by palbociclib displayed strong differences between *RB1*-mutant and wt cells as described above, *in silico* analyses revealed that the downregulated genes were FOXM1 targets. FOXM1 is a transcriptional activator with multiple oncogenic roles (41) that was identified as a critical phosphorylation target in a proteomic analysis of potential substrates of CDK4 kinase (27). In agreement, we also observed that the treatment with palbociclib or knockdown of CDK4 led to reduced FOXM1 phosphorylation, supporting the relevance of FOXM1 to maintain the oncogenic properties of cancer cells and its relevance in solid tumors (41). In addition, we provide evidence indicating that inactivation of RB1 promotes the activation of FOXM1 in bladder cancer cells. It has been proposed that FOXM1 confers resistance to chemotherapeutic agents, including CDDP, as supported by our current data. Importantly, as CDDP is the gold standard for bladder cancer management (6), our findings suggest that the *in vivo* treatment with palbociclib would allow reducing CDDP doses, possibly allowing the treatment of the patients with "unfit" bladder cancer. In fact, using xenografts, we found a tumor regression in the combined treatment, while CDDP

alone had no major effect. Similar findings also linking FOXM1 with CDDP resistance/sensitivity have been reported for other solid tumors (42). We further provide evidence that FOXM1 expression, and phosphorylated FOXM1 levels, dictates resistance or sensitivity to CDDP *in vitro* in bladder cancer cells. Of note, we also observed that the reduction of CDK4 levels did not affect CDDP sensitivity, indicating that under these conditions, CDDP sensitivity is not dependent on FOXM1, as we observed that the knockdown of CDK4 impinges FOXM1 phosphorylation and produces the reduction FOXM1 levels. Although the molecular mechanisms dependent on CDK4 levels or its kinase activity that may govern sensitivity to CDDP are presently unknown, it is possible to speculate that, in the absence of CDK4, cyclin D is released and may act through a CDK4-independent manner to sustain CDDP sensitivity. Importantly, the relationship between cyclin D levels and sensitivity to CDDP and other chemotherapeutic agents has been reported in other cell types (43–45). In addition, we observed that palbociclib induced p27 in all cell lines. Such induction, directly (46) or through the transcriptional modulation (47) of Fanconi genes (48) or AURKA (49), may contribute to this effect. In addition, the reduced EZH2 expression observed in the transgenic mouse model, or activity, as shown by reduced EZH2 Thr 487 phosphorylation, may increase CDDP sensitivity (50). These possibilities, in the context of FOXM1 expression and activity on its possible impact of CDDP and palbociclib sensitivity and the dependence of RB status, would be the subject of future research.

To further support these previous findings in cultured bladder cancer cells and their derived xenografts, we analyzed the treatment effects in a new *in vivo* metastatic bladder cancer mouse model (QKO), in which multiple genes involved in bladder cancer are inactivated ($Rb1^{F/F}$;*Rbl1-/-*; $Trp53^{F/F}$; $Pten^{F/F}$). The same approach using adenovirus coding for Cre recombinase has been previously validated showing that *Pten* and *Trp53* loss is sufficient to cause invasive bladder cancer (19), whereas the complete ablation of retinoblastoma family (Rb, p107, and p130) induces high-risk NMIBC in mice (20). Using our QKO model, we found high-grade and invasive tumors with metastatic spreading, affecting the liver, lungs, and the peritoneal cavity, really similar to that observed in metastatic human bladder cancer (51). In agreement with our previous findings with cells, the combined treatment was highly effective. In addition, the transcriptome analyses revealed the reversion of gene patterns characteristics of the tumor cells. The transcriptome analyses also demonstrated a reduced *EZH2* expression and a downregulation of FOXM1 phosphorylation. These findings could be attributed to the repression of activating E2Fs, and in particular E2F3a, already identified as main regulators of *EZH2* expression in bladder cancer (20). In addition, treated tumors showed high immune cell infiltration. This observation has a great relevance given the recent evidences in breast cancer models, indicating that CDK4/6 inhibitors may trigger antitumor immune response (52). Moreover, there have been positive results in clinical trials with immune checkpoint inhibitors, although still limited to a low percentage of patients in bladder cancer (53). Therefore, it will be important to ascertain whether palbociclib, alone or in combination with CDDP, could confer increased sensitivity to immune checkpoint inhibitors, increasing the percentage of patients who could benefit from these therapies.

Finally, based on our results and to consider CDK4/6 inhibitors for the stratified management of bladder cancer, we also analyzed the association of FOXM1 expression and outcome. Our data revealed that the increased activity and expression of FOXM1 in NMIBC identifies primary tumors at high risk of recurrence, and the possibility that these tumors display invasive characteristics in the recurrences. These data support the previous FOXM1-dependent gene signature related to recurrence in bladder cancer (54). Moreover, integrative global genomic analyses of advanced bladder cancer supported its relevance (10, 11).

As a whole, our data represent the rational basis for possible future clinical trials in patients with bladder cancer. These observations collectively support the relevance of palbociclib, alone or in combination with other therapeutics, to be a tool for the clinical management of advanced bladder cancer. Our results also show the main role of FOXM1 in human patients with bladder cancer, and how its phosphorylation-mediated activation could identify patients of poor clinical outcome. In addition, our data open new possible avenues for combined treatments, particularly in cases where the patient's condition would not support the conventional use of CDDP-based chemotherapy and currently present limited treatment options.

Disclosure of Potential Conflicts of Interest

D. Castellano is a consultant/advisory board member for Astra Zeneca, Bayer, Bristol-Myers Squibb, Janssen, Pfizer, and Roche. No potential conflicts of interest were disclosed by the other authors.

Authors' Contributions

Conception and design: C. Rubio, F. Villacampa, D. Castellano, J.M. Paramio
Development of methodology: C. Rubio, M. Martínez-Fernández, C. Segovia, I. Lodewijk, C. Segrelles, E. Munera-Maravilla, M. Santos, F. Guerrero-Ramos, D. Castellano, J.M. Paramio
Acquisition of data (provided animals, acquired and managed patients, provided facilities, etc.): C. Rubio, M. Martínez-Fernández, C. Segovia, I. Lodewijk, C. Suarez-Cabrera, F. López-Calderón, E. Munera-Maravilla, M. Santos, A. Bernardini, C. Lorz, M. José Gómez-Rodriguez, G. De Velasco, F. Villacampa, F. Guerrero-Ramos, S. Ruiz, F. de la Rosa, F.X. Real, M. Dueñas, J.M. Paramio
Analysis and interpretation of data (e.g., statistical analysis, biostatistics, computational analysis): C. Rubio, M. Martínez-Fernández, C. Suarez-Cabrera, C. Segrelles, F. López-Calderón, R. García-Escudero, G. De Velasco, S. Domínguez-Rodríguez, F.X. Real, N. Malats, D. Castellano, M. Dueñas, J.M. Paramio
Writing, review, and/or revision of the manuscript: C. Rubio, M. Martínez-Fernández, C. Segovia, I. Lodewijk, E. Munera-Maravilla, A. Bernardini, C. Lorz, M. José Gómez-Rodriguez, G. De Velasco, F. Villacampa, F.X. Real, N. Malats, D. Castellano, M. Dueñas, J.M. Paramio
Administrative, technical, or material support (i.e., reporting or organizing data, constructing databases): C. Rubio, C. Suarez-Cabrera, C. Segrelles, I. Otero, J.M. Paramio
Study supervision: C. Rubio, D. Castellano, J.M. Paramio
Other (review and revision of the manuscript): M. Santos

Acknowledgments

We express our deepest acknowledgement to patients and their families. We acknowledge Dr. A. Gandarillas [Institute of Research Marqués de Valdecilla (IDIVAL), Santander, Spain] for providing us FOXM1-coding plasmid and to Pilar Hernández, Raquel Ruiz-Palomares, and Jorge Peral for their help with experimental procedures. We also acknowledge Pfizer SLU for providing us palbociclib. This work was supported by FEDER cofounded MINECO grant SAF2015-66015-R, ISCIII-RETIC RD12/0036/0009, and PIE 15/00076 and CB/16/00228 (to J.M. Paramio); FEDER cofounded MINECO ISCIII grant PI15/00993 (to M. Santos); FEDER cofounded MINECO grants SAF2013-49147-P and SAF2016-80874-P and Ramon y Cajal contract RYC-2011-09242 (to S. Ruiz); and a grant from Asociación Española contra el Cáncer

(AECC; to F.X. Real, D. Castellano, and N. Malats). This work was also partially supported by a Pfizer preclinical grant (CTP WI235570; to J.M. Paramio).

The costs of publication of this article were defrayed in part by the payment of page charges. This article must therefore be hereby marked *advertisement* in accordance with 18 U.S.C. Section 1734 solely to indicate this fact.

Received March 3, 2018; revised June 20, 2018; accepted September 18, 2018; published first September 21, 2018.

References

1. Jemal A, Bray F, Center MM, Ferlay J, Ward E, Forman D. Global cancer statistics. CA Cancer J Clin 2011;61:69–90.
2. Knowles MA, Hurst CD. Molecular biology of bladder cancer: new insights into pathogenesis and clinical diversity. Nat Rev Cancer 2015;15:25–41.
3. Burger M, Oosterlinck W, Konety B, Chang S, Gudjonsson S, Pruthi R, et al. ICUD-EAU International Consultation on Bladder Cancer 2012: Non-muscle-invasive urothelial carcinoma of the bladder. Eur Urol 2013;63: 36–44.
4. van Rhijn BW, Burger M, Lotan Y, Solsona E, Stief CG, Sylvester RJ, et al. Recurrence and progression of disease in non-muscle-invasive bladder cancer: from epidemiology to treatment strategy. Eur Urol 2009;56: 430–42.
5. Stenzl A, Cowan NC, De Santis M, Kuczyk MA, Merseburger AS, Ribal MJ, et al. Treatment of muscle-invasive and metastatic bladder cancer: update of the EAU guidelines. Eur Urol 2011;59:1009–18.
6. Witjes JA, Comperat E, Cowan NC, De Santis M, Gakis G, Lebret T, et al. EAU guidelines on muscle-invasive and metastatic bladder cancer: summary of the 2013 guidelines. Eur Urol 2014;65:778–92.
7. Bellmunt J, de Wit R, Vaughn DJ, Fradet Y, Lee JL, Fong L, et al. Pembrolizumab as second-line therapy for advanced urothelial carcinoma. N Engl J Med 2017;376:1015–26.
8. Rosenberg JE, Hoffman-Censits J, Powles T, van der Heijden MS, Balar AV, Necchi A, et al. Atezolizumab in patients with locally advanced and metastatic urothelial carcinoma who have progressed following treatment with platinum-based chemotherapy: a single-arm, multicentre, phase 2 trial. Lancet 2016;387:1909–20.
9. Powles T, Eder JP, Fine GD, Braiteh FS, Loriot Y, Cruz C, et al. MPDL3280A (anti-PD-L1) treatment leads to clinical activity in metastatic bladder cancer. Nature 2014;515:558–62.
10. Cancer Genome Atlas Research Network. Comprehensive molecular characterization of urothelial bladder carcinoma. Nature 2014;507:315–22.
11. Robertson AG, Kim J, Al-Ahmadie H, Bellmunt J, Guo G, Cherniack AD, et al. Comprehensive molecular characterization of muscle-invasive bladder cancer. Cell 2017;171:540–56.
12. Clark AS, Karasic TB, DeMichele A, Vaughn DJ, O'Hara M, Perini R, et al. Palbociclib (PD0332991)-a selective and potent cyclin-dependent kinase inhibitor: a review of pharmacodynamics and clinical development. JAMA Oncol 2016;2:253–60.
13. Earl J, Rico D, Carrillo-de-Santa-Pau E, Rodriguez-Santiago B, Mendez-Pertuz M, Auer H, et al. The UBC-40 Urothelial Bladder Cancer cell line index: a genomic resource for functional studies. BMC Genomics 2015;16:403.
14. Fry DW, Harvey PJ, Keller PR, Elliott WL, Meade M, Trachet E, et al. Specific inhibition of cyclin-dependent kinase 4/6 by PD 0332991 and associated antitumor activity in human tumor xenografts. Mol Cancer Ther 2004;3: 1427–38.
15. Owczarek TB, Kobayashi T, Ramirez R, Rong L, Puzio-Kuter AM, Iyer G, et al. ARF confers a context-dependent response to chemotherapy in muscle-invasive bladder cancer. Cancer Res 2017;77:1035–46.
16. Costa C, Santos M, Segrelles C, Duenas M, Lara MF, Agirre X, et al. A novel tumor suppressor network in squamous malignancies. Sci Rep 2012;2:828.
17. Moral M, Segrelles C, Lara MF, Martinez-Cruz AB, Lorz C, Santos M, et al. Akt activation synergizes with Trp53 loss in oral epithelium to produce a novel mouse model for head and neck squamous cell carcinoma. Cancer Res 2009;69:1099–108.
18. Ramirez A, Bravo A, Jorcano JL, Vidal M. Sequences 5′ of the bovine keratin 5 gene direct tissue- and cell-type-specific expression of a lacZ gene in the adult and during development. Differentiation 1994;58:53–64.
19. Puzio-Kuter AM, Castillo-Martin M, Kinkade CW, Wang X, Shen TH, Matos T, et al. Inactivation of p53 and Pten promotes invasive bladder cancer. Genes Dev 2009;23:675–80.
20. Santos M, Martinez-Fernandez M, Duenas M, Garcia-Escudero R, Alfaya B, Villacampa F, et al. In vivo disruption of an Rb-E2F-Ezh2 signaling loop causes bladder cancer. Cancer Res 2014;74:6565–77.
21. Costa C, Santos M, Martinez-Fernandez M, Duenas M, Lorz C, Garcia-Escudero R, et al. E2F1 loss induces spontaneous tumour development in Rb-deficient epidermis. Oncogene 2013;32:2937–51.
22. Bornachea O, Santos M, Martinez-Cruz AB, Garcia-Escudero R, Duenas M, Costa C, et al. EMT and induction of miR-21 mediate metastasis development in Trp53-deficient tumours. Sci Rep 2012;2:434.
23. Duenas M, Martinez-Fernandez M, Garcia-Escudero R, Villacampa F, Marques M, Saiz-Ladera C, et al. PIK3CA gene alterations in bladder cancer are frequent and associate with reduced recurrence in non-muscle invasive tumors. Mol Carcinog 2015;54:566–76.
24. Maraver A, Fernandez-Marcos PJ, Cash TP, Mendez-Pertuz M, Duenas M, Maietta P, et al. NOTCH pathway inactivation promotes bladder cancer progression. J Clin Invest 2015;125:824–30.
25. VanArsdale T, Boshoff C, Arndt KT, Abraham RT. Molecular pathways: targeting the cyclin D-CDK4/6 axis for cancer treatment. Clin Cancer Res 2015;21:2905–10.
26. Kuleshov MV, Jones MR, Rouillard AD, Fernandez NF, Duan Q, Wang Z, et al. Enrichr: a comprehensive gene set enrichment analysis web server 2016 update. Nucleic Acids Res 2016;44:W90–7.
27. Anders L, Ke N, Hydbring P, Choi YJ, Widlund HR, Chick JM, et al. A systematic screen for CDK4/6 substrates links FOXM1 phosphorylation to senescence suppression in cancer cells. Cancer Cell 2011;20:620–34.
28. Hu CJ, Wang B, Tang B, Chen BJ, Xiao YF, Qin Y, et al. The FOXM1-induced resistance to oxaliplatin is partially mediated by its novel target gene Mcl-1 in gastric cancer cells. Biochim Biophys Acta 2015;1849:290–9.
29. Chou TC. Drug combination studies and their synergy quantification using the Chou-Talalay method. Cancer Res 2010;70:440–6.
30. Ruiz S, Santos M, Segrelles C, Leis H, Jorcano JL, Berns A, et al. Unique and overlapping functions of pRb and p107 in the control of proliferation and differentiation in epidermis. Development 2004;131:2737–48.
31. Subramanian A, Tamayo P, Mootha VK, Mukherjee S, Ebert BL, Gillette MA, et al. Gene set enrichment analysis: a knowledge-based approach for interpreting genome-wide expression profiles. Proc Natl Acad Sci U S A 2005;102:15545–50.
32. Martinez-Fernandez M, Rubio C, Segovia C, Lopez-Calderon FF, Duenas M, Paramio JM. EZH2 in bladder cancer, a promising therapeutic target. Int J Mol Sci 2015;16:27107–32.
33. Gormally MV, Dexheimer TS, Marsico G, Sanders DA, Lowe C, Matak-Vinkovic D, et al. Suppression of the FOXM1 transcriptional programme via novel small molecule inhibition. Nat Commun 2014;5:5165.
34. Sanders DA, Gormally MV, Marsico G, Beraldi D, Tannahill D, Balasubramanian S. FOXM1 binds directly to non-consensus sequences in the human genome. Genome Biol 2015;16:130.
35. Czachorowski MJ, Amaral AF, Montes-Moreno S, Lloreta J, Carrato A, Tardon A, et al. Cyclooxygenase-2 expression in bladder cancer and patient prognosis: results from a large clinical cohort and meta-analysis. PLoS One 2012;7:e45025.
36. Chiron D, Di Liberto M, Martin P, Huang X, Sharman J, Blecua P, et al. Cell-cycle reprogramming for PI3K inhibition overrides a relapse-specific C481S BTK mutation revealed by longitudinal functional genomics in mantle cell lymphoma. Cancer Discov 2014;4:1022–35.
37. Gao Y, Shen J, Choy E, Mankin H, Hornicek F, Duan Z. Inhibition of CDK4 sensitizes multidrug resistant ovarian cancer cells to paclitaxel by increasing apoptosiss. Cell Oncol 2017;40:209–18.
38. Rivadeneira DB, Mayhew CN, Thangavel C, Sotillo E, Reed CA, Grana X, et al. Proliferative suppression by CDK4/6 inhibition: complex function of the retinoblastoma pathway in liver tissue and hepatoma cells. Gastroenterology 2010;138:1920–30.

39. Sage J, Miller AL, Perez-Mancera PA, Wysocki JM, Jacks T. Acute mutation of retinoblastoma gene function is sufficient for cell cycle re-entry. Nature 2003;424:223–8.
40. Wang H, Nicolay BN, Chick JM, Gao X, Geng Y, Ren H, et al. The metabolic function of cyclin D3-CDK6 kinase in cancer cell survival. Nature 2017;546:426–30.
41. Li L, Wu D, Yu Q, Li L, Wu P. Prognostic value of FOXM1 in solid tumors: a systematic review and meta-analysis. Oncotarget 2017;8:32298–308.
42. Kwok JM, Peck B, Monteiro LJ, Schwenen HD, Millour J, Coombes RC, et al. FOXM1 confers acquired cisplatin resistance in breast cancer cells. Mol Cancer Res 2010;8:24–34.
43. Zhen Y, Fang W, Zhao M, Luo R, Liu Y, Fu Q, et al. miR-374a-CCND1-pPI3K/AKT-c-JUN feedback loop modulated by PDCD4 suppresses cell growth, metastasis, and sensitizes nasopharyngeal carcinoma to cisplatin. Oncogene 2017;36:275–85.
44. Iizuka S, Oridate N, Nashimoto M, Fukuda S, Tamura M. Growth inhibition of head and neck squamous cell carcinoma cells by sgRNA targeting the cyclin D1 mRNA based on TRUE gene silencing. PLoS One 2014;9: e114121.
45. Zhou X, Zhang Z, Yang X, Chen W, Zhang P. Inhibition of cyclin D1 expression by cyclin D1 shRNAs in human oral squamous cell carcinoma cells is associated with increased cisplatin chemosensitivity. Int J Cancer 2009;124:483–9.
46. Zhang Y, Yu JJ, Tian Y, Li ZZ, Zhang CY, Zhang SF, et al. eIF3a improve cisplatin sensitivity in ovarian cancer by regulating XPC and p27Kip1 translation. Oncotarget 2015;6:25441–51.
47. Pippa R, Espinosa L, Gundem G, Garcia-Escudero R, Dominguez A, Orlando S, et al. p27Kip1 represses transcription by direct interaction with p130/E2F4 at the promoters of target genes. Oncogene 2012;31:4207–20.
48. Plimack ER, Dunbrack RL, Brennan TA, Andrake MD, Zhou Y, Serebriiskii IG, et al. Defects in DNA repair genes predict response to neoadjuvant cisplatin-based chemotherapy in muscle-invasive bladder cancer. Eur Urol 2015;68:959–67.
49. Xu J, Yue CF, Zhou WH, Qian YM, Zhang Y, Wang SW, et al. Aurora-A contributes to cisplatin resistance and lymphatic metastasis in non-small cell lung cancer and predicts poor prognosis. J Transl Med 2014;12:200.
50. Riquelme E, Suraokar M, Behrens C, Lin HY, Girard L, Nilsson MB, et al. VEGF/VEGFR-2 upregulates EZH2 expression in lung adenocarcinoma cells and EZH2 depletion enhances the response to platinum-based and VEGFR-2-targeted therapy. Clin Cancer Res 2014;20:3849–61.
51. Kamat AM, Hahn NM, Efstathiou JA, Lerner SP, Malmstrom PU, Choi W, et al. Bladder cancer. Lancet 2016;388:2796–810.
52. Goel S, DeCristo MJ, Watt AC, BrinJones H, Sceneay J, Li BB, et al. CDK4/6 inhibition triggers anti-tumour immunity. Nature 2017;548:471–5.
53. Bellmunt J, Powles T, Vogelzang NJ. A review on the evolution of PD-1/PD-L1 immunotherapy for bladder cancer: The future is now. Cancer Treat Rev 2017;54:58–67.
54. Kim SK, Roh YG, Park K, Kang TH, Kim WJ, Lee JS, et al. Expression signature defined by FOXM1-CCNB1 activation predicts disease recurrence in non-muscle-invasive bladder cancer. Clin Cancer Res 2014;20:3233–43.
55. Chen EY, Tan CM, Kou Y, Duan Q, Wang Z, Meirelles GV, et al. Enrichr: interactive and collaborative HTML5 gene list enrichment analysis tool. BMC Bioinformatics 2013;14:128.
56. Bergamaschi A, Madak-Erdogan Z, Kim YJ, Choi YL, Lu H, Katzenellenbogen BS. The forkhead transcription factor FOXM1 promotes endocrine resistance and invasiveness in estrogen receptor-positive breast cancer by expansion of stem-like cancer cells. Breast Cancer Res 2014;16:436.